Cryobiology 115 (2024) 104894

Contents lists available at ScienceDirect

Cryobiology

journal homepage: www.elsevier.com/locate/cryo

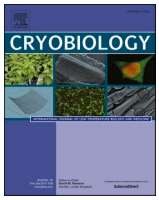

In vivo study of porous NiTi cryotweezers for bone tissue cryotherapy

Ekaterina S. Marchenko [a], Kirill M. Dubovikov [a], Ivan I. Kuzhelivskiy [b], Maksim O. Pleshkov [c], Evgeniy S. Koroluk [c], Konstantin S. Brazovskii [d,e], Alex A. Volinsky [a,f,*]

[a] Laboratory of Superelastic Biointerfaces, National Research Tomsk State University, 36 Lenin Ave., 634045, Tomsk, Russia
[b] Department of Pediatric Surgical Diseases, Siberian State Medical University, 72 Olega Koshevogo Str., 634050, Tomsk, Russia
[c] Laboratory "Bionic Digital Platforms", Siberian State Medical University, 2c7 Moskovsky Trakt, 634050, Tomsk, Russia
[d] Division of Medical and Biological Cybernetics, Department of Biomedicine, Siberian State Medical University, 2 Moskovsky Trakt, 634050, Tomsk, Russia
[e] Research School of Chemistry & Applied Biomedical Sciences, Tomsk Polytechnic University, Tomsk, Russia
[f] Department of Mechanical Engineering, University of South Florida, 4202 E. Fowler Ave. ENG030, Tampa, FL, 33620, USA

ARTICLE INFO

Keywords:
NiTi
Cryotherapy
Liquid nitrogen
Cryoapplicator
Cryotweezers

ABSTRACT

This study examined the effects of liquid nitrogen vapor on osteogenesis in the rabbit femur. Cryotweezers made of porous nickel titanium alloy (nitinol or NiTi) obtained by self-propagating high temperature synthesis were used in this experiment. The porous structure of the cryotweezers allows them to hold up to 10 g of liquid nitrogen after being immersed for 2 min, which completely evaporates after 160 s. To study the effects of liquid nitrogen evaporation on osteogenesis, a rabbit femur was perforated. The formed holes were subjected to cryotherapy with varying exposure times. It was found that a 3 s exposure time stimulates osteogenesis, which was manifested in a greater number of osteoblasts in the regenerate compared to the control sample without liquid nitrogen. It was observed that increasing the exposure to 6, 9 or 12 s had a destructive effect, to varying degrees. The most severe damage was exerted by a 12 s exposure, which resulted in the formation of osteonecrosis areas. In the samples exposed to 6 and 9 s of cryotherapy, destruction of the cytoplasm of osteocytes and osteoclasts was observed.

1. Introduction

Due to technological development, minimally invasive surgeries have become an alternative to classical surgical procedures solving a number of medical problems. For example, cryodestruction or cryoablation is one of the approaches used in cryosurgery to remove skin tumors and to treat heart arrhythmias by exposing tissues to extremely low temperatures [2,14]. While metals and alloys are classic materials for cryoinstruments, there are reports of cryoapplicators made from sapphire single crystals [22]. There are multiple papers that demonstrate the successful treatment of various diseases using refrigerants in cryosurgery [2,6,14,22]. For example, in Ref. [6], a cryosurgical operation was performed to remove osteosarcoma in a child's knee, followed by reconstruction with a vascularized peroneal graft. The authors of the study reported the absence of complications after surgery and the attainment of good functional properties. Removal of warts using cryodestruction is another fairly common type of minimally invasive surgery [2]. Cryodestruction has also been used for the treatment of malignant and benign tumors of the liver [4,8], prostate [20,24], kidney [3,23], breast [7,21], skin [13,27], and bones [6].

NiTi alloys are a popular choice for making cryosurgical instruments, largely due to their high biocompatibility and corrosion resistance [11,15,16,26]. The physical and mechanical properties of NiTi make it a promising material in medical applications. Cooling NiTi to liquid nitrogen temperature does not lead to its embrittlement unlike ceramic or polymer materials. Another feature of NiTi is that it does not stick to the affected tissues during the procedure, so there is no need to heat the instrument to safely detach it from the tissue. The operating principle of a porous NiTi cryoapplicator is based on the capillary effect, which has been studied in detail in many papers, especially using cryogenic liquids [5,30,32,33]. The essence of this phenomenon is that when a liquid is absorbed into a porous structure, it is retained due to capillary forces. It was experimentally established that the optimal pore size is 90–120 μm [33]. Liquid nitrogen is retained inside the NiTi cryoapplicator and gradually evaporates, producing vapor used in cryotherapy, which is confirmed by testing procedures [10]. Thus, cryotherapy occurs due to the impact of liquid nitrogen steam absorbed in porous structure of NiTi cryotweezers and touching tissue with metal cooled to ~196 °C, which

* Corresponding author. Laboratory of Superelastic Biointerfaces, National Research Tomsk State University, 36 Lenin Ave., 634045, Tomsk, Russia
E-mail address: volinsky@usf.edu (A.A. Volinsky).

https://doi.org/10.1016/j.cryobiol.2024.104894
Received 25 December 2023; Received in revised form 28 March 2024; Accepted 10 April 2024
Available online 17 April 2024
0011-2240/Published by Elsevier Inc. on behalf of Society for Cryobiology.

leads to instant heat dissipation from the tissue surface [10].

Why did we choose nitinol made by self-propagating high temperature synthesis (SHS) as a material for cryotweezers? The choice of the material for cryotweezers was made for a number of reasons. First, the SHS technology is quite simple and does not require anything other than powder and inert gas to create an ingot, from which the active element for cryotweezers is cut out. Second, it is known that the material can corrode upon contact with body tissues. NiTi undergoes passivation, which has a positive effect on its corrosion resistance [18]. Third, NiTi does not stick to tissues and mucous membranes at cryogenic temperatures. This is ensured by a corrosion-resistant, refractory oxynitride layer, which is formed on the surface of the porous alloy during SHS [12,31]. Therefore, the use of nitinol obtained by SHS as an active element in cryotweezers is quite promising. The features described above distinguish cryotweezers made of nitinol from those made by Brymill Cryogenic Systems, for example. The handles of the Brymill Cryogenic Systems cryotweezers are made of stainless steel, the tips are made of brass, and the entire tweezers are Teflon-coated [1].

Cold exposure has been shown to have an effect on osteoarticular tissue, including potentiating the development of cartilage tissue and osteohistogenesis processes. Cryoregenerative treatment has been the subject of many research papers focusing on pathologies such as skeletal bone fractures, osteoporosis of the knee joints, osteochondrosis of the spine, etc. [9,17,29]. The purpose of this work is to enhance osteogenesis in rabbit bones through cryotherapy using porous NiTi cryotweezers.

2. Materials and methods

The SHS method makes it possible to obtain NiTi with 30–70 % porosity by controlling the synthesis process parameters. Titanium PTOM-2 and nickel PNK OT-4 powders were used for the production of cryoinstruments. SHS was carried out in the layer-by-layer combustion mode in a flow reactor with an atmosphere containing both argon and nitrogen. The mixture consisted of 44.9 wt% Ti and 55.1 wt% Ni powders to obtain a mixture of 50 at.% Ti and 50 at.% Ni. This mixture was poured into a quartz tube and placed in a reactor. The sample was heated to 350–380 °C before ignition. The gases were fed into the reactor at 0.01–0.05 MPa pressure. The samples were ignited with a hot molybdenum electric coil. The output was NiTi cylinders with 60–70 % porosity. Active elements for cryotweezers were made from porous SHS-NiTi, shown in Fig. 1. These active elements were cut out from a porous ingot by electrical discharge machining.

The surface structure of porous NiTi was studied using scanning electron microscopy (SEM, Thermo Fisher Scientific, USA, Axia ChemiSEM), in the secondary electron detection mode. The measurements were conducted using 10–20 kV accelerating voltage, 100 mA beam current, 10 Pa vacuum, and 4.5–6 μm spot size.

The research study investigated the effects of liquid nitrogen evaporation on osteogenesis using three rabbits of the “chinchilla” breed. The rabbits used in the study were of both sexes and were at least 6 months old and their weights ranged from 2.7 to 3.5 kg after a 15-day quarantine period before the start of the experiment. Three other rabbits of the “chinchilla” breed were also used as control group. Their bones were not treated by liquid nitrogen. Samples of the resulting regenerate were stained with hematoxylin-eosin. The study was performed using an Axio Lab A1 optical microscope (Carl Zeiss, Germany, Oberkochen) and MIRAX MIDI scanner (Carl Zeiss, Germany, Oberkochen). Ultrathin sections were prepared according to Weekley’s method [25] with a thickness of 60–100 nm using an Ultrotome III (LKB, Sweden, Stockholm). Staining was carried out with uranyl acetate and lead citrate without spraying. The samples were investigated using a JEM-100 CXII electron microscope (JEOL, Japan, Akishima, Tokyo) with 25–30 μm spot size operated at 80 kV.

Fig. 2 shows the full surgery process. The surgery was performed under general anesthesia by intramuscular administration of the

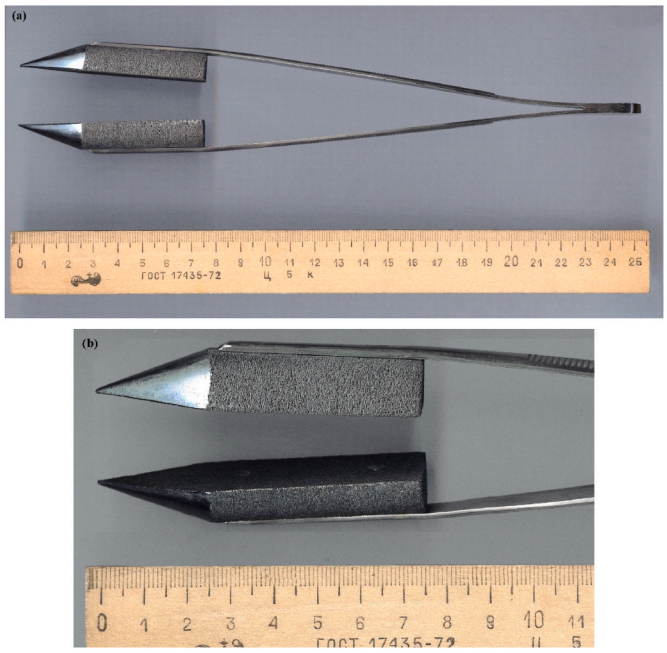

Fig. 1. (a) General view of the cryotweezer; (b) Active element made from porous SHS-NiTi.

Zoletil® 100 drug at a dosage of 15 mg/kg, with preliminary premedication with 0.1 % atropine sulfate solution at a dosage of 0.1 ml subcutaneously. The surgical field was shaved under general anesthesia as shown in Fig. 2(a) and a direct incision up to 9 cm long was made in the animal’s skin. This incision was made in the projection of the left femur. The thigh muscles were exfoliated in Fig. 2(b). After injecting the muscles in the surgical wound area with 5 ml 0.5 % Novocain solution, access to the femur was made along the diaphysis. Four 3 mm diameter holes were made with an electric drill along the femoral shaft 1 cm apart from the proximal to the distal parts of the bone in Fig. 2(c) and (d). Cryotherapy was carried out with a special applicator made of porous NiTi cryotweezers in Fig. 1. The cryotweezers were immersed in liquid nitrogen for 30 s and then were placed in each hole from the proximal edge. Different exposure times were applied to each hole: the first hole – 3 s, the second hole – 6 s, the third – 9 s, and the fourth hole – 12 s in Fig. 2(e). This protocol was followed to investigate the influence of exposure time of the refrigerant on the cryodestruction process within the bone tissue. The wound closure was performed in layers and the skin in the postoperative suture area was treated with an antiseptic in Fig. 2 (f). The antibiotic Cefazolin was introduced intramuscularly. The animal smoothly emerged from anesthesia, and was provided with water and standard postoperative animal care.

The studies were carried out according to the requirements of the Declaration of Helsinki for the Treatment of Animals [28] and in strict accordance with the International Ethical and Scientific Standards for the Quality of Planning and Conducting Animal Research [19]. The experiments were performed in compliance with the order of the Ministry of Health of the USSR No. 176 dated August 12, 1977. The Ethics Committee of the Siberian State Medical University approved the research work presented in this paper based on the protocol titled “Surgical treatment of dysplastic diseases using cryotechnologies and titanium nickelide implants” (experimental part) and found it to be compliant with ethical standards and regulatory rules (registration 4669/1, dated March 21, 2016). The experimental studies were conducted in the laboratory of biological models of the Siberian State Medical University.

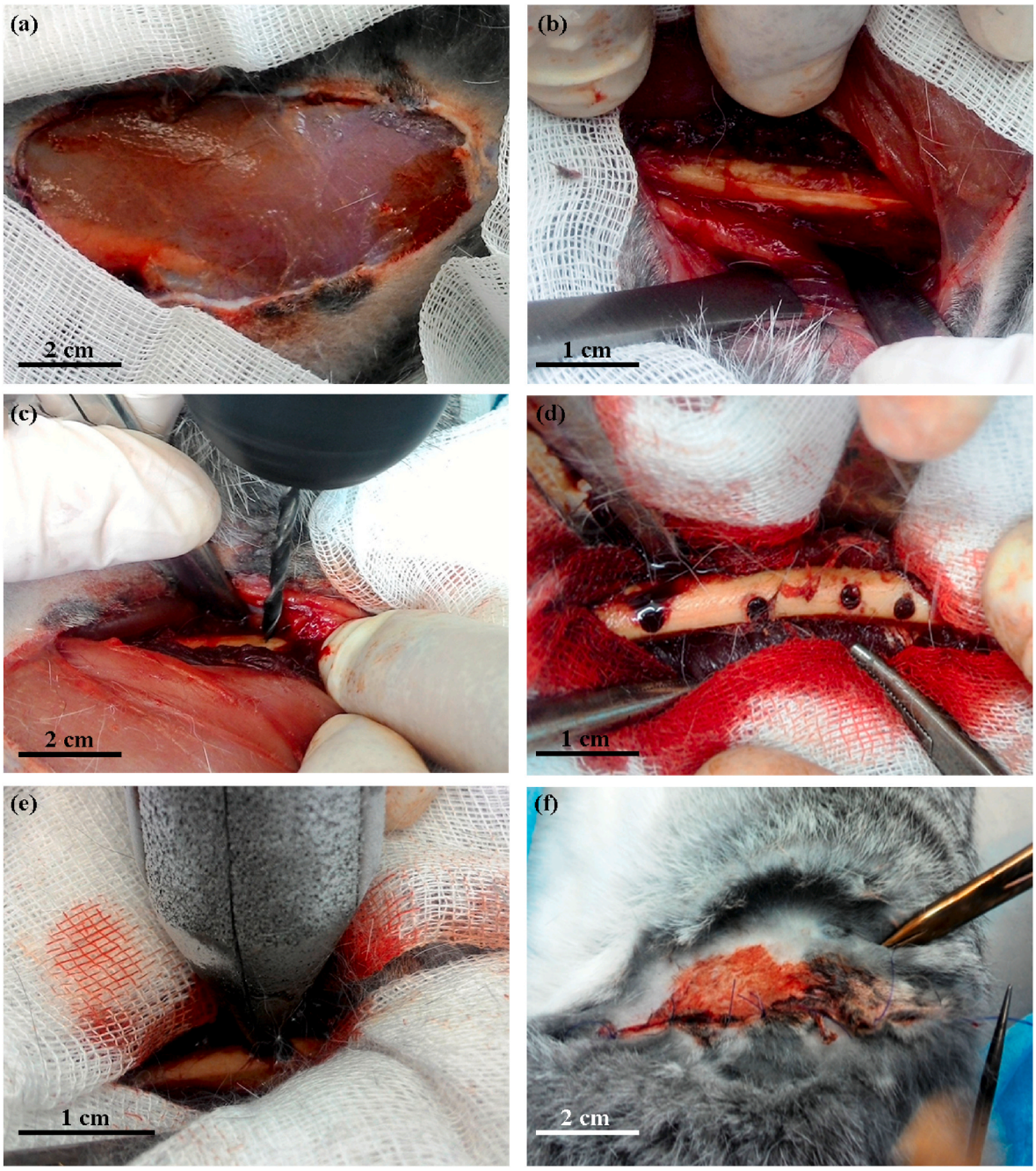

Fig. 2. Surgery for introducing refrigerant into the femur; (a) Initial surgical wound; (b) Surgical wound after access to the femur; (c), (d) Making burr holes in the femur; (e) Cryotreatment of burr holes in the diaphysis of the femur; (f) Postoperative suture of the right thigh area.

3. Results and discussion

Fig. 3 shows SEM images of porous SHS NiTi with ~60 % porosity. Randomly oriented bridges ranging from 50 μm to 200 μm in size are visible on the section plane in Fig. 3(a). A high level of porosity is a feature of this material, which allows it to be used as a container for refrigerant. The fracture surface cross-section demonstrates the presence of a thin layer on the bridges in Fig. 3(b). This layer contains titanium oxycarbonitrides formed during synthesis. The layer thickness is about 1.3 μm, and it provides a good level of corrosion protection. While this slightly affects the shape memory and superelasticity of the alloy, these properties are not relevant for cryotweezers because they are not mechanically deformed during the procedure. The pore distribution histogram shows that the vast majority of pores are smaller than 200 μm, confirmed by the SEM images in Fig. 3. The presence of individual bridges larger than 500 μm is also worth noting.

To obtain time-dependent coolant supply, a simple weighing experiment was conducted three times. The weight of cryotweezers without coolant is 109.3 g. Using an electronic scale, it was determined that after immersing the cryotweezers in liquid nitrogen for 2 min, their weight increased by 9–10 g as shown in Fig. 4. For every 3 s of liquid nitrogen evaporation, the weight decreased by 0.3 g. After 12 s, approximately 1 g of coolant was released. After 1 min, half of the absorbed liquid nitrogen had evaporated. At 2 min and 40 s, all liquid nitrogen had evaporated from the cryotweezers as its weight decreased to the original 109.3–109.5 g.

After a ten-day rehabilitation period, another surgical procedure was performed on the animals to collect organic material for

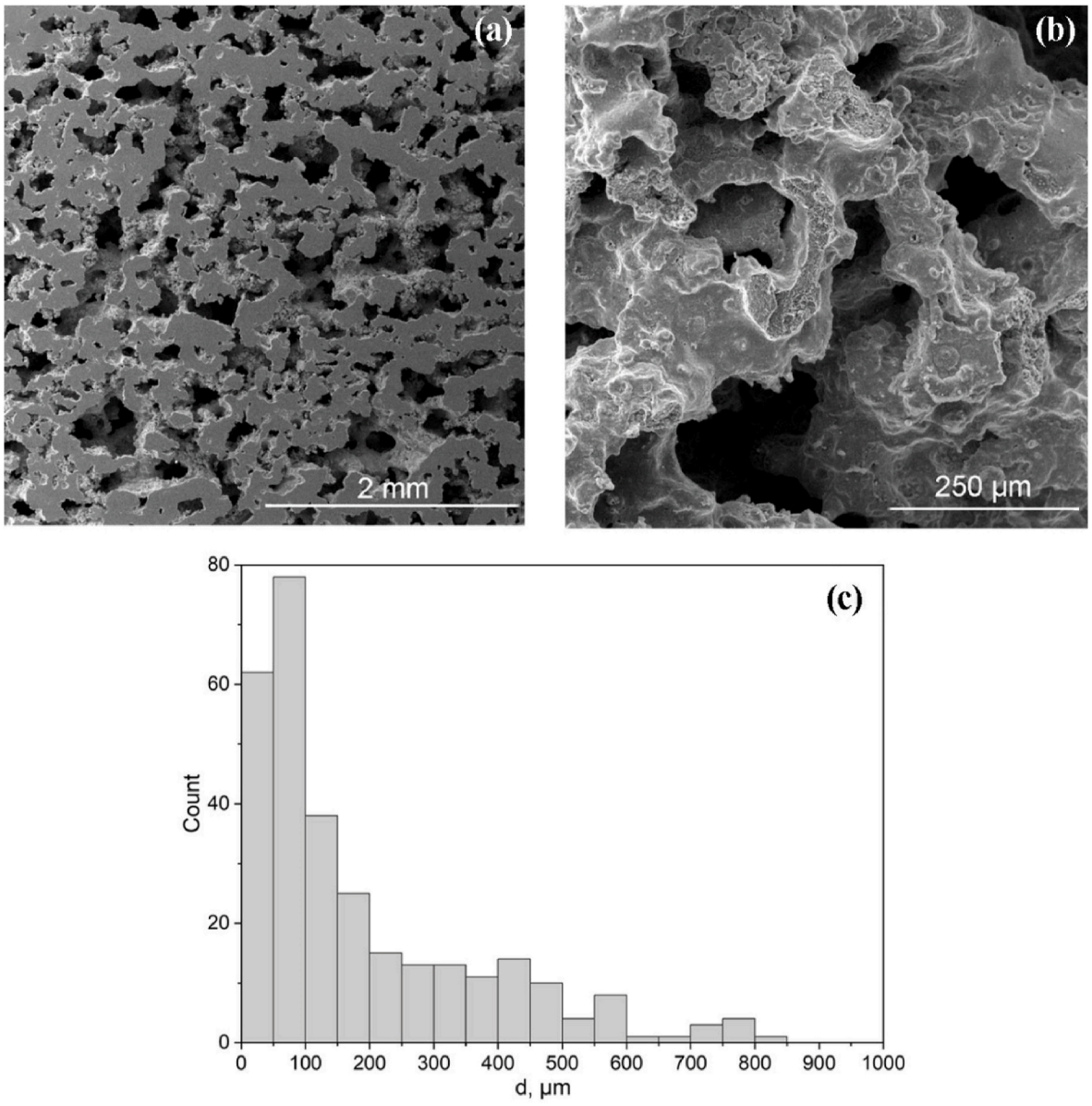

Fig. 3. SEM images of SHS-NiTi with ~60 % porosity: (a) Polished surface; (b) Fracture surface; (c) Histogram of the pore size distribution.

histomorphological studies to establish the influence of cryotherapy on osteogenesis. The animal's condition was normal during the post-operative period in Fig. 5(a). The surgical intervention proceeded smoothly and the animal's condition corresponds to the severity of the surgery. The wound healed by secondary intention. On the 10th day post-surgery, the formed scar was excised intraoperatively under anesthesia. After excising the scar tissue, access to the femur was achieved and a revision of the bone diaphysis was performed as shown in Fig. 5 (b). Upon visual examination, the burr holes with 3 s, 6 s, and 9 s coolant exposure showed less pronounced destructive changes. In contrast, the area of the burr hole with a 12 s exposure showed pronounced gray-brown densely elastic whitish layers. These layers resemble necrosis. The samples for histology and SEM were obtained using an Optimum scalpel and a Volkmann micro-spoon from each of four burr holes in Fig. 5(c).

In addition to the collection of the cryoregenerate, the regenerate was taken from the hole without cryotherapy (control group) in Fig. 6. A histomorphological study of the regenerate from the control group revealed the usual formation of primary callus through the development of cartilage and connective tissue. A similar microscopic examination demonstrated typical processes of osteohistogenesis because the single chondrocytes (black arrows in Fig. 6(b)) were observed in the sample.

Optical microscopy of the cryoregenerate with a 3 s coolant exposure demonstrates very active calcification of the regenerate. Primary callus consists of fibrous and reticulofibrous tissue. The regenerate is represented by chains of osteoblasts. There are no signs of destruction in Fig. 7.

The results of optical microscopy of cryoregenerates with a 6 s and 9 s exposure time are presented in Fig. 8. Optical microscopy of tissue with a 6 s exposure to a coolant revealed the presence of single osteoblasts, callus formation, development of cartilaginous tissue, and predominance of connective tissue as shown in Fig. 8(a). The optical image of the tissue sample exposed to the coolant for 9 s mainly shows connective tissue in Fig. 8(b). It can be concluded, based on the analysis of the histiocytic reaction in the 6 s and 9 s regenerates that cryodestruction was quite active, as there are no osteoblasts and a low content of cartilage tissue.

Optical microscopy results of tissue with a 12 s coolant exposure are shown in Fig. 9(a). Optical microscopy of the tissue sample exposed to the coolant for 12 s reveals abundant connective tissue development, as

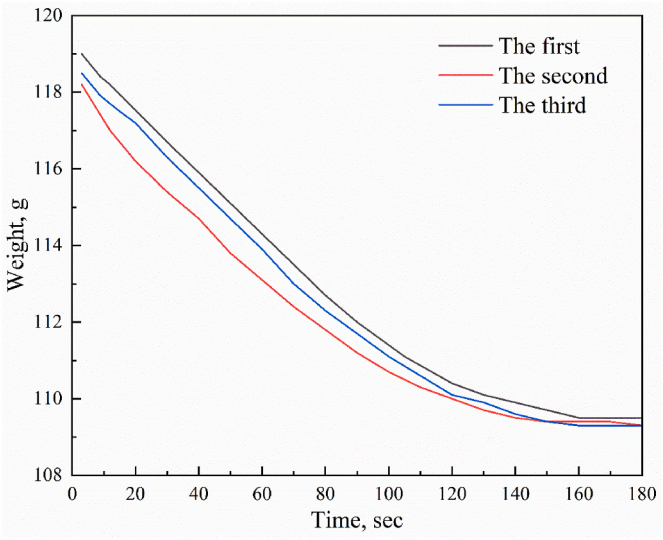

Fig. 4. Time-dependent coolant supply after immersing in liquid nitrogen for 2 min. The weight of cryotweezers without liquid nitrogen is 109.3 g. The experiment was repeated three times.

evidenced by the absence of blood vessels. The histomorphological picture resembles the development of connective tissue after cryonecrosis. A tissue sample exposed for 12 s showed moderate fibroblast proliferation and moderate lymphoid infiltration in Fig. 9(b).

The images of 5–7 μm thick sections obtained by optical microscopy are presented in Fig. 10. In a tissue sample that was not subjected to cryotherapy, a pronounced proliferation of osteoblasts is observed in Fig. 10(a). Extensive areas are observed in which a large number of osteoblasts are present, distributed uniformly. The sample subjected to cryotherapy with a 3 s exposure shows a significantly higher number of osteoblasts compared to the control group in Fig. 10(b). Osteoblasts are distributed uniformly, and there are no areas in which osteoblasts aren't observed. It can be concluded that exposure of coolant for 3 s had a positive effect on osteogenesis, accelerating it. Osteoblast proliferation for 6 s and 9 s exposure samples was observed in Fig. 10(c and d), but to a much lesser degree compared to the control group or sample with a 3 s exposure. Therefore, it can be assumed that cryotherapy with 6 and 9 s exposure slows down osteogenesis, and probably has a destructive effect on the structure of osteoblasts.

In order to study the degree of destruction, SEM images of the regenerates were obtained. A typical picture of osteocyte, formed during osteoregeneration without cryotherapy is shown in Fig. 11(a). The SEM images of a sample with 3 s exposure reveal a large number of osteoblasts, the cytoplasm of which is rich in cisterns of the endoplasmic reticulum and mitochondria, which may indicate active synthetic activity and remodeling of the bone matrix. The cells are surrounded by a large number of collagen fibers and a relatively homogeneous intercellular matrix. An osteoblast is pointed to with a white arrow in Fig. 11(b). The cytoplasm of the osteocytes was destructed in the regenerate with 6 s exposure in Fig. 11(c). The destructed cytoplasm is characterized by changes in the mitochondrial cristae, the appearance of a significant number of vacuoles in the cytoplasm, and a significant expansion of the

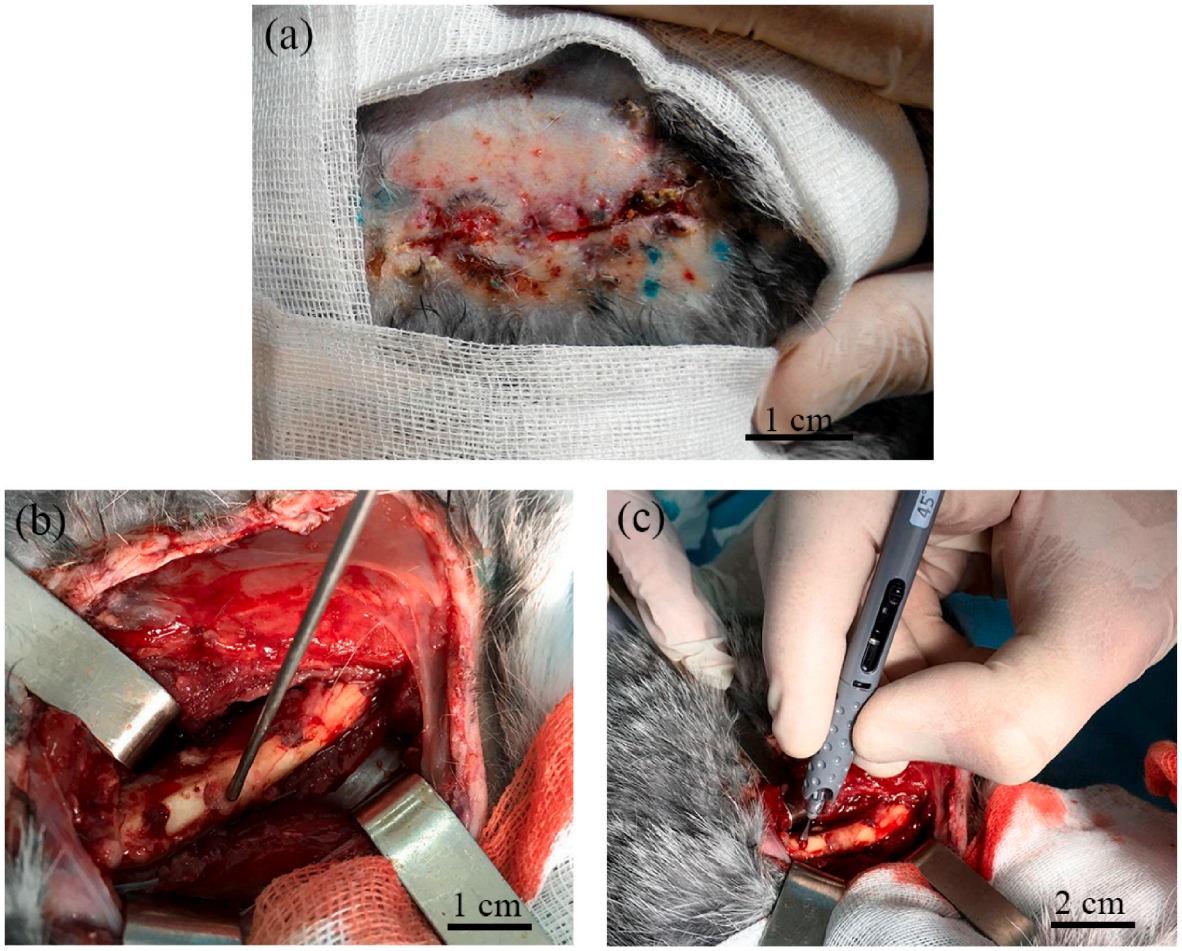

Fig. 5. Obtaining material for histomorphological studies: (a) Postoperative scar of the right thigh on the 10th day after surgery; (b) Destructive deposits in the area of the hole with a 9 s coolant exposure; (c) Tissue sampling from the burr holes of the femur on the 10th day after cryotherapy.

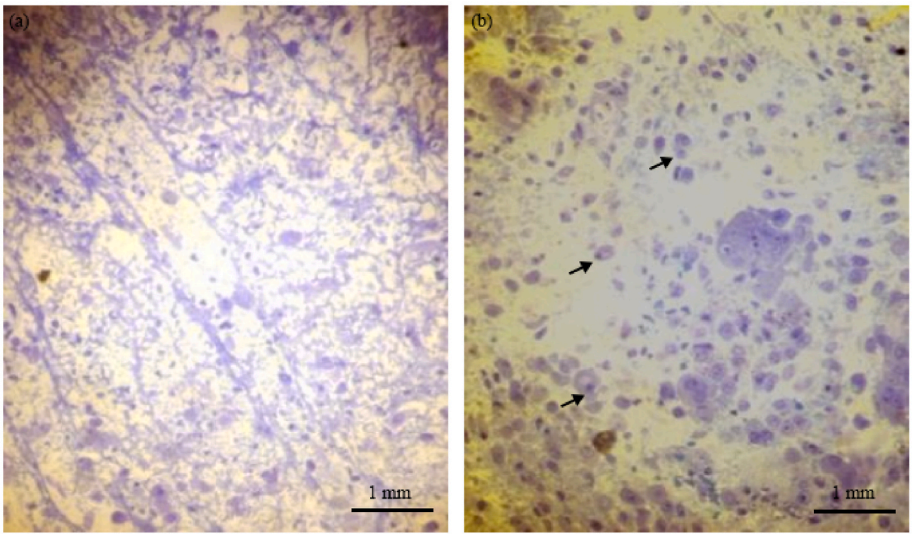

Fig. 6. Structural changes in the tissue of an animal in the control group: (a) Formation of cartilage and connective tissue and (b) Single chondrocytes. Here, the black arrows point to single chondrocytes.

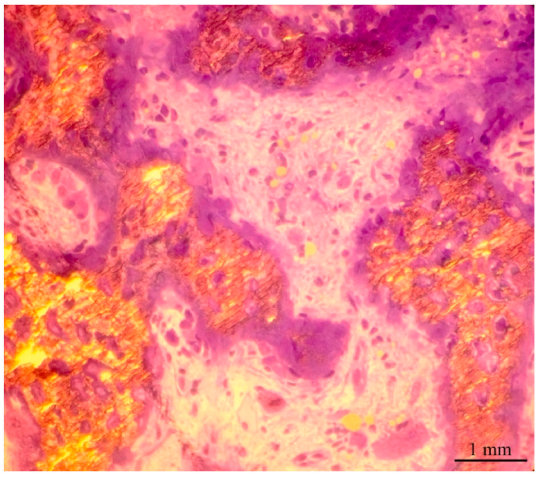

Fig. 7. Optical image of a thinned tissue section with a 3 s coolant exposure.

endoplasmic reticulum cisterns. The surrounding matrix is heterogeneous. Collagen fibers are characterized by disorientation. The regenerate with a 9 s exposure revealed that osteoclasts are characterized by hyperchromic cytoplasm, which is filled with vacuoles and inclusions of various sizes as shown in Fig. 11(d). This indicates significant damage and bone resorption. The intercellular substance is heterogeneous. Collagen fibers experienced destruction phenomena. Comparing the structure of the osteocyte that arose during the natural regeneration of the control group with the osteocytes of the samples with 6 and 9 s exposure, their pronounced destruction is observed. The 3 s cryoexposure not only had a positive effect on the proliferation of osteoblasts in Fig. 10(b), but also didn't have any destructive effects on cellular organelles in Fig. 11(b).

Marginal condensation of chromatin is observed in osteocytes at the microscopic level. The cytoplasm of cells is hyperchromic and contains a large number of vacuoles and dilated endoplasmic reticulum cisternae. The mitochondrial apparatus is poor and subject to destructive changes. The intercellular substance is characterized by the disorientation of

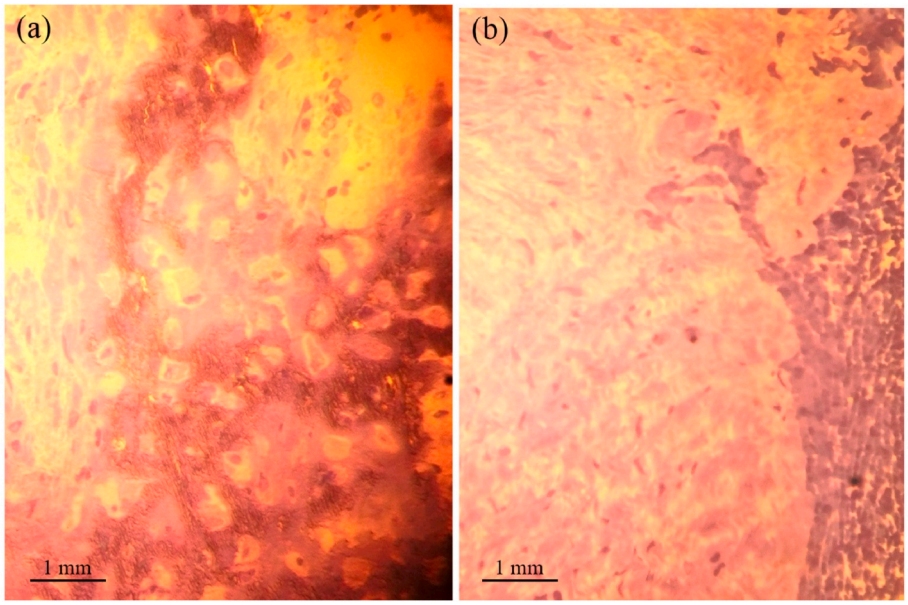

Fig. 8. Optical images of thinned tissue sections exposed to coolant for: (a) 6 s and (b) 9 s.

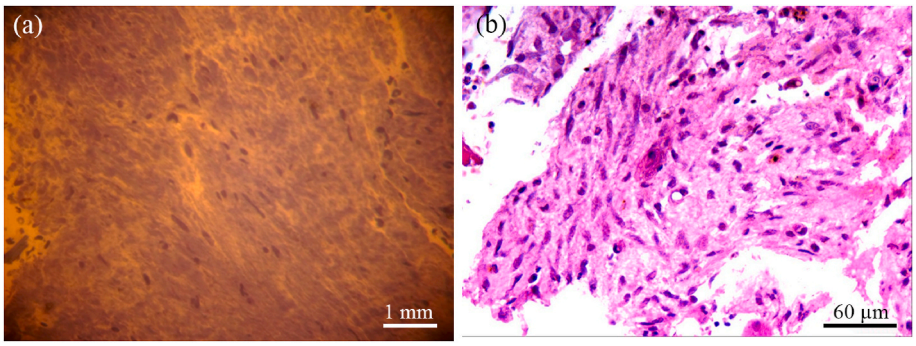

Fig. 9. Optical images of tissue with a 12 s exposure: (a) Thin section and (b) Moderate fibroblast proliferation and moderate lymphoid infiltration.

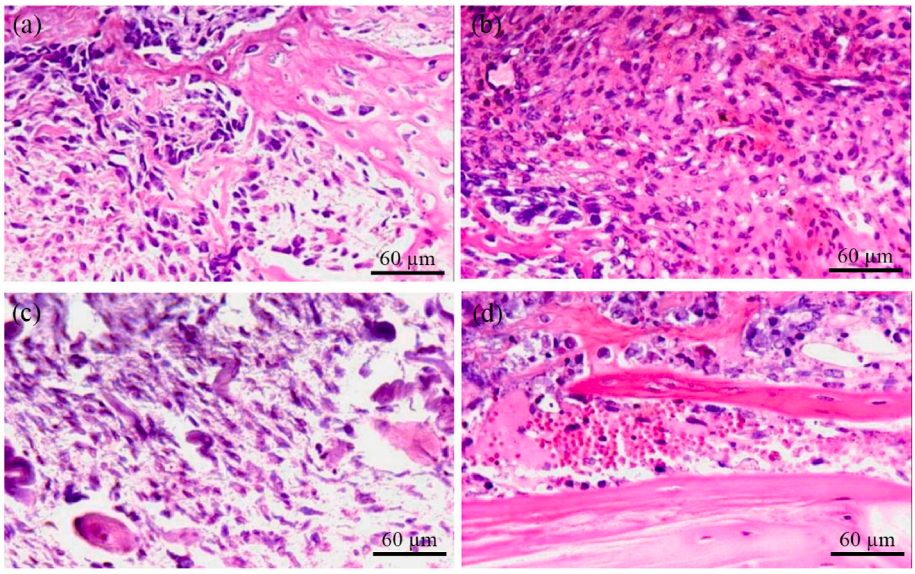

Fig. 10. The images obtained by optical microscopy of the samples: (a) Without cryo-influence; (b) After 3 s of cryotherapy; (c) After 6 s of cryotherapy; (d) After 9 s of cryotherapy.

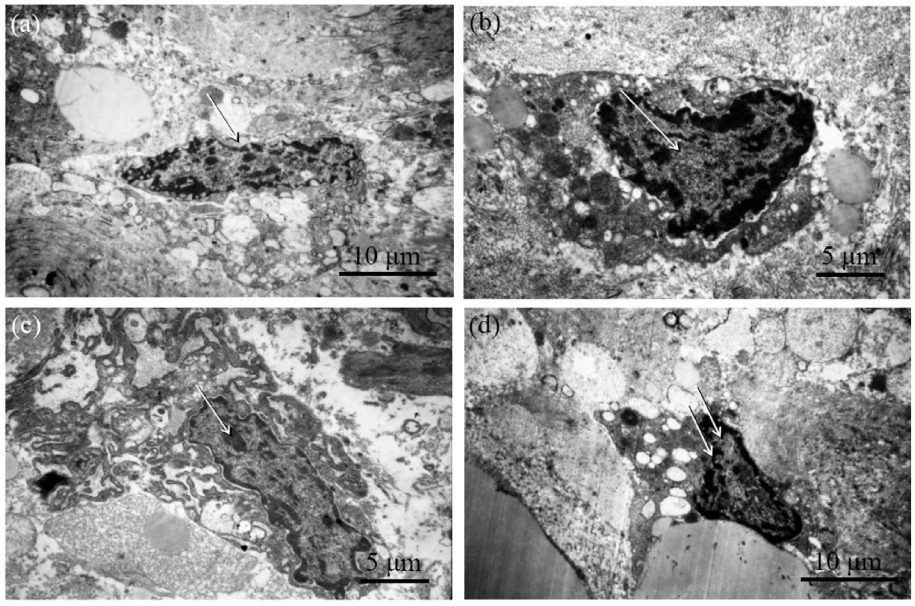

Fig. 11. SEM images of the regenerates from the holes: (a) Without cryo-influence. Osteocyte (white arrow); (b) After 3 s of cryotherapy. Osteoblast (white arrow); (c) After 6 s of cryotherapy. Osteocyte (white arrow); (d) After 9 s of cryotherapy. Osteocyte (white arrow) with vacuolated cytoplasm.

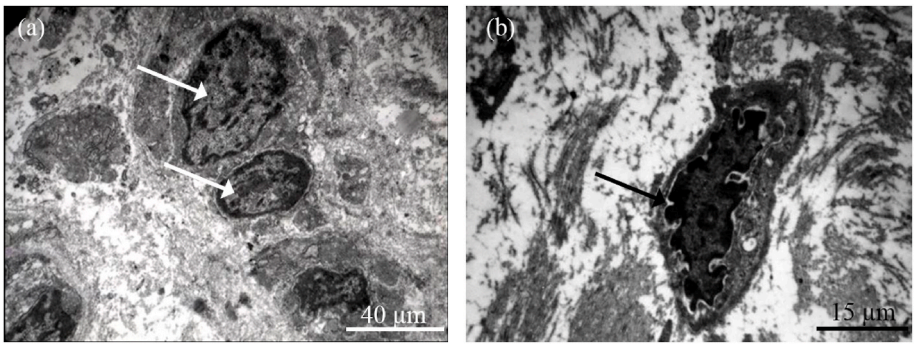

Fig. 12. SEM images of: (a) 12 s cryotherapy osteonecrosis zone. Osteoblasts (white arrows) with hyperchromic cytoplasm and violation of the orientation of collagen fibers in the intercellular space; (b) Osteonecrosis zone (black arrow) with cryotherapy.

collagen fibers and inhomogeneous matrix density in Fig. 12(a). An osteocyte with hyperchromic vacuolated cytoplasm is observed in Fig. 12(b). There is a significant violation of the architectonics of collagen fibers in the intercellular substance.

Electron microscopy of ultrathin sections also demonstrates the destruction processes manifested by the hyperchromia of the osteoblast cytoplasm, the expansion of the cisterns of the endoplasmic reticulum, and the disruption of the architectonics of collagen fibers and the concentration of intercellular components. An optical microscopy morphological study was carried out using histological preparations stained with hematoxylin and eosin 10 days after experiments. The macroscopic study revealed more pronounced destructive changes in the cut holes with coolant treatment for 12 s compared to exposures of 6 s and 9 s. In contrast to the 12 s exposure group, the cut holes subjected to 6 s and 9 s coolant exposure did not exhibit distinct development of connective tissue. Thus, the pronounced cryonecrosis after a 12 s refrigerant exposure exhibited qualitative differences compared with other modes, therefore, additional morphometric quantitative assessments were not required. The most preferable cryotherapy mode is with a 3 s exposure because the cryoregenerate demonstrated active calcification represented by chains of osteoblasts compared with the control group, where typical processes of osteohistogenesis were observed.

The conclusion that a 3 s exposure is optimal is made only for this study. A shorter cryotherapy of 1 or 2 s may either have an equally positive effect on osteogenesis. In addition, since in this study a rabbit femur with a thickness of 7–9 mm was subjected to cryotherapy, for thinner bones a 3 s exposure can lead to their destruction. Therefore, it is necessary to take into account the properties of bones before cryotherapy.

4. Conclusions

The NiTi alloy produced through the SHS method offers a novel approach to the manufacture and use of cryoinstruments due to its high heat capacity and ductility, which provide rapid local cooling and its ability to prevent sticking to moist mucous tissues. The developed porous structure of the cryoinstrument consists of small and large pores allowing the refrigerant (liquid nitrogen) to be retained inside the tool providing cryotherapy due to the impact of liquid nitrogen vapor as it evaporates and cool metal coming into contact with the tissue surface. This leads to instant heat dissipation from the tissue surface. An in vivo study conducted with rabbit bones showed that the optimal exposure time of cryotherapy is 3 s because active calcification occurs. Increasing exposure time leads to the destruction of bone tissue. The most destructive signs, such as the formation of osteonecrosis areas were observed in the regenerate after a 12 s exposure. At the same time, it was observed that a 6 s and 9 s exposure resulted in the destruction of the cytoplasm of osteocytes and osteoclasts, respectively. These results have potential implications for the therapy of various bone diseases, such as osteogenesis imperfecta.

CRediT authorship contribution statement

Ekaterina S. Marchenko: Conceptualization, Data curation, Funding acquisition, Investigation, Project administration, Resources, Supervision. **Kirill M. Dubovikov:** Formal analysis, Methodology, Software, Validation, Visualization, Writing – original draft, Data curation, Investigation, Resources. **Ivan I. Kuzhelivskiy:** Data curation, Formal analysis, Investigation, Methodology, Resources, Validation, Visualization. **Maksim O. Pleshkov:** Data curation, Formal analysis, Investigation, Methodology, Validation, Visualization. **Evgeniy S. Koroluk:** Data curation, Formal analysis, Investigation, Methodology, Resources, Validation. **Konstantin S. Brazovskii:** Conceptualization, Formal analysis, Investigation, Methodology, Resources, Validation, Visualization. **Alex A. Volinsky:** Data curation, Formal analysis, Methodology, Resources, Visualization, Writing – review & editing.

Declaration of competing interest

The authors declare that they have no known competing financial interests or personal relationships that could have appeared to influence the work reported in this paper.

Acknowledgments

This research was supported by the Russian Science Foundation Grant No. 19-72-10105, https://rscf.ru/project/19-72-10105/.

References

[1] W. Abramovits, Cryotweezers, in: W. Abramovits, G. Graham, Y. Har-Shai, R. Strumia (Eds.), Dermatological Cryosurgery and Cryotherapy, Springer, London, 2016, pp. 129–130.
[2] T. Anzai, A. Tsunoda, Yu Saikawa, F. Matsumoto, Sh Ito, K. Ikeda, Cryosurgical ablation for treatment of common warts on the nasal vestibule, Am. J. Otolaryngol. 41 (2020) e102641, https://doi.org/10.1016/j.amjoto.2020.102641.
[3] J.G. Baust, K.K. Snyder, K.L. Santucci, A.T. Robilotto, R.G. Van Buskirk, J.M. Baust, Cryoablation: physical and molecular basis with putative immunological consequences, Int. J. Hyperther. 36 (2019) 10–16, https://doi.org/10.1080/02656736.2019.1647355.
[4] C. Cha, F.T.Jr. Lee, L.F. Rikkers, J.E. Niederhuber, B.T. Nguyen, D.M. Mahvi, Rationale for the combination of cryoablation with surgical resection of hepatic tumors, J. Gastrointest. Surg. 5 (2001) 206–213, https://doi.org/10.1016/s1091-255x(01)80034-2.
[5] S.W. Choi, W.I. Lee, H.S. Kim, Analysis of flow characteristics of cryogenic liquid in porous media, Int. J. Heat Mass Tran. 87 (2015) 161–183, https://doi.org/10.1016/j.ijheatmasstransfer.2015.03.066.
[6] U.S. Erwin, S.D. Cahyadi, Cryosurgery and vascularized fibular graft reconstruction in proximal tibia osteosarcoma in young children: a case report, Int. J. Surg. Case Rep. 89 (2021) e106568, https://doi.org/10.1016/j.ijscr.2021.106568.
[7] R.E. Fine, R.C. Gilmore, J.R. Dietz, S.K. Boolbol, M.P. Berry, L.K. Han, A.S. Kenler, M. Sabel, K.R. Tomkovich, N.A. VanderWalde, M. Chen, K.S. Columbus, L. D. Curcio, S.M. Feldman, L. Gold, L. Hernandez, E.R. Manahan, S.A. Seedman, R. P. Vaidya, A.B. Sevrukov, H.D. Aoun, R.D. Hicks, R.M. Simmons, Cryoablation without excision for low-risk early-stage breast cancer: 3-year interim analysis of ipsilateral breast tumor recurrence in the ICE3 trial, Ann. Surg Oncol. 28 (2021) 5525–5534, https://doi.org/10.1245/s10434-021-10501-4.

[8] W. Gao, Z. Guo, X. Zhang, Y. Wang, W. Zhang, X. Yang, H. Yu, Percutaneous cryoablation of ovarian cancer metastasis to the liver: initial experience in 13 patients, Int. J. Gynecol. Cancer 25 (2015) 802–808, https://doi.org/10.1097/IGC.0000000000000420.

[9] I.C.M. van der Geest, M.P. van Noort, H.W.B. Schreuder, M. Pruszczynski, J.W.J. de Rooy, R.P.H. Veth, The cryosurgical treatment of chondroblastoma of bone: long-term oncologic and functional results, J. Surg. Oncol. 96 (2007) 230–234, https://doi.org/10.1002/jso.20804.

[10] V.E. Gunther, Delay Law and New Class of Materials and Implants in Medicine, first ed., STT Publishing, Tomsk, 2000.

[11] N.J. Hallab, K.J. Bundy, K. O'Connor, R.L. Moses, J.J. Jacobs, Evaluation of metallic and polymeric biomaterial surface energy and surface roughness characteristics for directed cell adhesion, Tissue Eng. 71 (2001) 55–71, https://doi.org/10.1089/107632700300003297.

[12] O.V. Kokorev, V.N. Khodorenko, G.A. Baigonakova, E.S. Marchenko, YuF. Yasenchuk, V.E. Gunther, S.G. Anikeev, G.A. Barashkova, Metal-glass-ceramic phases on the surface of porous NiTi-based SHS-material for carriers of cells, Russ. Phys. J. 61 (2019) 1734–1738, https://doi.org/10.1007/s11182-018-1594-0.

[13] E.G. Kuflik, Cryosurgery for skin cancer: 30-year experience and cure rates, Dermatol. Surg. 30 (2004) 297–300, https://doi.org/10.1111/j.1524-4725.2004.30090.x.

[14] K. Kwak, B. Yu, R.J. Lewandowski, D.H. Kim, Recent progress in cryoablation cancer therapy and nanoparticles mediated cryoablation, Theranostics 12 (2022) 2175–2204, https://doi.org/10.7150/thno.67530.

[15] E. Marchenko, G. Baigonakova, K. Dubovikov, O. Kokorev, Y. Yasenchuk, A. Vorozhtsov, In vitro bio-testing comparative analysis of NiTi porous alloys modified by heat treatment, Metals 12 (2022) e1006, https://doi.org/10.3390/met12061006.

[16] K. Mehta, K. Gupta, Fabrication and Processing of Shape Memory Alloys, first ed., Springer International Publishing, Cham, Switzerland, 2019 https://doi.org/10.1007/978-3-319-99307-2.

[17] I. Meller, A. Weinbroum, J. Bickels, S. Dadia, A. Nirkin, O. Merimsky, J. Issakov, G. Flusser, N. Marouani, N. Cohen, Y. Kollender, Fifteen years of bone tumor cryosurgery: a single-center experience of 440 procedures and long-term follow-up, Eur. J. Surg. Oncol. 34 (2008) 921–927, https://doi.org/10.1016/j.ejso.2007.11.001.

[18] M. Mirjalili, M. Momeni, N. Ebrahimi, M.H. Moayed, Comparative study on corrosion behaviour of Nitinol and stainless steel orthodontic wires in simulated saliva solution in presence of fluoride ions, Mater. Sci. Eng. C 33 (4) (2013) 2084–2093, https://doi.org/10.1016/j.msec.2013.01.026.

[19] National committee for research ethics in science and technology (NENT), guidelines for research ethics in science and technology, JWE 14 (2009) 255–266, https://doi.org/10.1515/9783110208856.255.

[20] P.J. Pasricha, S. Hill, K.S. Wadwa, G.T. Gislason, P.I. rd Okolo, C.A. Magee, M. I. Canto, W.H. Kuo, J.G. Baust, A.N. Kalloo, Endoscopic cryotherapy: experimental results and first clinical use, Gastrointest. Endosc. 49 (1999) 627–631, https://doi.org/10.1016/s0016-5107(99)70393-7.

[21] S.O. Pfleiderer, M.G. Freesmeyer, C. Marx, R. Kuhne-Heid, A. Schneider, W. A. Kaiser, Cryotherapy of breast cancer under ultrasound guidance: initial results and limitations, Eur. Radiol. 12 (2002) 3009–3014, https://doi.org/10.1007/s00330-002-1511-2.

[22] I.A. Shikunova, I.N. Dolganova, A.A. Kuznetsov, E.E. Mukhina, L.P. Safonova, K. I. Zaytsev, V.N. Kurlov, Sapphire crystal cryoapplicators enabling control of cryosurgery based on light-tissue interaction, Cryobiology 92 (2020) 278–279, https://doi.org/10.1016/j.cryobiol.2019.11.032.

[23] S. Sriprasad, M. Aldiwani, S. Pandian, T.K. Nielsen, M. Ismail, N.J. Barber, G. Lughezzani, A. Larcher, B.W. Lagerveld, F.X. Keeley Jr., Renal function loss after cryoablation of small renal masses in solitary kidneys: European registry for renal cryoablation multi-institutional study, J. Endourol. 34 (2020) 233–239, https://doi.org/10.1089/end.2019.0669.

[24] C. Sze, E. Tsivian, K.J. Tay, A.A. Schulman, L.G. Davis, R.T. Gupta, T.J. Polascik, Anterior gland focal cryoablation: proof-of-concept primary prostate cancer treatment in select men with localized anterior cancers detected by multi-parametric magnetic resonance imaging, BMC Urol. 19 (2019) e127, https://doi.org/10.1186/s12894-019-0562-5.

[25] B.S. Weakley, A Beginner's Handbook in Biological Electron Microscopy, Churchill Livingstone, London, England, 1972.

[26] A.H. Weshahy, R.M. Abdel Hay, D. Metwally, O.A. Weshahy, Z. Gad, The efficacy of intralesional cryosurgery in the treatment of small- and medium-sized basal cell carcinoma: a pilot study, J. Dermatol. Treat. 26 (2015) 147–150, https://doi.org/10.3109/09546634.2014.906037.

[27] D.J. Wever, A.G. Veldhuizen, M.M. Sanders, J.M. Schakenraad, J.R. van Horn, Cytotoxic, allergic and genotoxic activity of a nickel-titanium alloy, J. Biomater. 18 (1997) 1115–1120, https://doi.org/10.1016/s0142-9612(97)00041-0.

[28] World Medical Association, World medical association declaration of Helsinki: ethical principles for medical research involving human subjects, JAMA 310 (2013) 2191–2194, https://doi.org/10.1001/jama.2013.281053.

[29] P.-K. Wu, C.-F. Chen, J.-Y. Wang, P.C.-H. Chen, M.-C. Chang, S.-C. Hung, W.-M. Chen, Freezing nitrogen ethanol composite may be a viable approach for cryotherapy of human giant cell tumor of bone, Clin. Orthop. Relat. Res. 475 (2017) 1650–1663, https://doi.org/10.1007/s11999-017-5239-3.

[30] R. Wu, M. Prat, Mass Transfer Driven Evaporation from Capillary Porous Media, first ed., CRC Press, Boca Raton, 2023.

[31] YuF. Yasenchuk, V.E. Gunther, E.S. Marchenko, T.L. Chekalkin, G.A. Bajgonakova, V.N. Khodorenko, S.V. Gyunter, J.H. Kang, S. Weiss, A. Obrosov, Formation of mineral phases in self-propagating high-temperature synthesis (SHS) of porous NiTi alloy, Mater. Res. Express 6 (2019) 1–13, https://doi.org/10.1088/2053-1591/ab01a1.

[32] M. Zhang, Capillary Transport of Cryogenic Liquids in Porous Structures, first ed., 2013. Cuvillier, Göttingen.

[33] Q. Zhu, W. Guo, R. Zhuan, P. Zhang, Cryogenic wicking of liquid nitrogen in the metallic screens with different weave densities, Int. J. Heat Mass Tran. 183 (2022) 122208, https://doi.org/10.1016/j.ijheatmasstransfer.2021.122208.